# Synthesis, Structure, and Properties of a Model for Galactose Oxidase

**Mei M. Whittaker, Walter R. Duncan, and James W. Whittaker***

Department of Chemistry, Carnegie Mellon University, 4400 Fifth Avenue, Pittsburgh, Pennsylvania 15213

*Received August 24, 1995*[⊗]

An active-site analog of the radical copper enzyme galactose oxidase has been prepared from a synthetic tripod chelate ((2-pyridylmethyl)[(2-hydroxy-3,5-dimethylphenyl)methyl][(2-hydroxy-5-methyl-3-(methylthio)phenyl)-methyl]amine, duncamine (dnc)) that binds a single Cu(II) ion through phenolate, thioether-substituted phenolate, and pyridylamine arms. The Cu complex crystallizes as a dinucleated dimer bridged by phenolate oxygens, and the structure has been determined by X-ray crystallography. Addition of pyridine (or other coordinating bases) dissociates the complex into a monomeric derivative that has been characterized spectroscopically (optical absorption and EPR) and electrochemically. The model provides insight into the properties of a mutant form of galactose oxidase which retains the same copper ligand complement as the wild type protein but lacks catalytic activity.

## Introduction

Galactose oxidase (EC 1.1.3.9) is a radical copper oxidase[1] that catalyzes the stereospecific oxidation of a broad range of alcohols to the corresponding aldehydes coupled with reduction of $O_2$ to $H_2O_2$.[2,3] Galactose oxidase is unusual among copper enzymes in appearing to catalyze two-electron-redox chemistry at a mononuclear active site. Previous work has shown that a free radical stabilized on a protein side chain participates directly in the redox chemistry as an additional redox site.[1,4−6] The crystal structure[7] of galactose oxidase shows the copper in a pyramidal site ligated to two equatorial histidine residues, two tyrosines (Y495 and Y272, in axial and equatorial positions, respectively), the remaining equatorial site being occupied by an acetate of crystallization, or a water molecule (see **1**). The structure reveals a novel biological modification of the equatorial tyrosine 272, which is covalently linked by a thioether bond to the sulfur atom of cysteine 228. Spectroscopic studies[6,8,9] of 2-(methylthio)-*p*-cresol, a model for this cross-linked amino acid, and its phenoxyl derivative have demonstrated that the modified tyrosine 272 is the free-radical redox site in galactose oxidase. Progress toward synthesis of a galactose oxidase model complex was recently reported with the preparation of a chelate bearing two pyridyl rings and a simple phenolic arm.[10] Here we report the synthesis and chacterization a galactose oxidase model compound containing a (methylthio)phenol group (mimicking the modified tyrosine−cysteine residue in the protein (Y272)), a dimethylphenol group (mimicking the unmodified tyrosine residue (Y495)), and a 2-(aminomethyl)pyridine group, together forming a tripod chelate that coordinates copper in an active-site-analog complex.

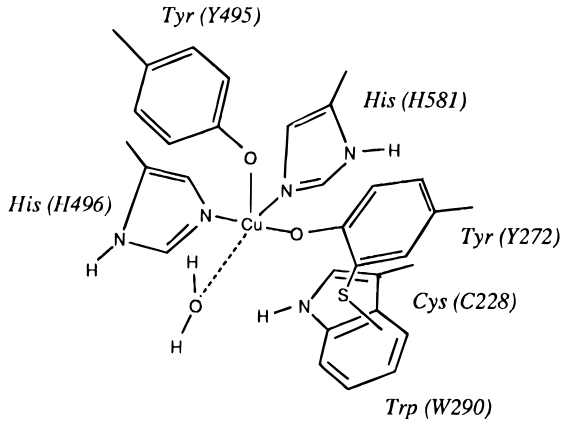


**1**

## Experimental Section

All reagents used in the preparation of complexes were obtained from commercial sources. When necessary, solvents used for synthesis were redistilled and stored under argon. Absorption spectra were recorded on a Varian Cary 5E UV−vis−near-IR spectrophotometer. EPR spectra were recorded on a Bruker ER300 EPR spectrometer equipped with an X-band microwave bridge and a nitrogen flow system. Quantitative EPR measurements were performed as previously described,[4] taking precautions to avoid power saturation of the EPR signal. EPR spectra were simulated using a standard program (SIM15, obtained from the Quantum Chemistry Program Exchange as QCPE265) modified to permit all nuclear hyperfine terms to be treated nonaxially. Electroanalytical measurements were obtained with an EG&G Model 263 potentiostat interfaced to a microcomputer for data acquisition and analysis. Cyclic voltammetry experiments were carried out in a standard three-electrode minicell with a glassy carbon or gold working electrode, a nonaqueous reference (Ag/0.1 M $AgNO_3$ in $CH_3CN$), and a Pt wire auxiliary electrode. Experiments were run with 0.1 M tetrabutylammonium tetrafluoroborate supporting electrolyte in $CH_2Cl_2$ or $CH_3CN$ with scan rates of 40 mV/s. Microanalyses were performed by Galbraith Laboratories, Knoxville, TN. Commercial crystal structure analyses were performed by Crystalytics Inc., Lincoln, NE.

* Corresponding author. Telephone 412-268-5670; FAX 412-268-6945; E-mail: jim@insight.chem.cmu.edu.

⊗ Abstract published in *Advance ACS Abstracts,* December 15, 1995.

(1) Whittaker, M. M.; Whittaker, J. W. *J. Biol. Chem.* **1990**, *265*, 9610−9613.
(2) Amaral, D.; Kelly-Falcoz, F.; Horecker, B. L. *Methods Enzymol.* **1966**, *9*, 87−92.
(3) Kosman, D. J. In *Copper Proteins and Copper Enzymes*; Lontie, R., Ed.; CRC Press, Inc.: Boca Raton, FL, 1984; Vol. 2, pp 1−26.
(4) Whittaker, M. M.; Whittaker, J. W. *J. Biol. Chem.* **1988**, *263*, 6074−6080.
(5) Whittaker, M. M.; DeVito, V. L.; Asher, S. A.; Whittaker, J. W. *J. Biol. Chem.* **1989**, *264*, 7104−7106.
(6) Babcock, G. T.; El-Deeb, M. K.; Sandusky, P. O.; Whittaker, M. M.; Whittaker, J. W. *J. Am. Chem. Soc.* **1992**, *114*, 3727−3734.
(7) Ito, N.; Phillips, S. E. V.; Stevens, C.; Ogel. Z. B.; Mcpherson, M. J.; Keen, J. N.; Yadav, K. D. S.; Knowles, P. F. *Nature* **1993**, *350*, 87−90.
(8) Itoh, S.; Hirano, K.; Furuta, A.; Komatsu, M.; Ohshiro, Y.; Ishida, A.; Takamuku, N.; Suzuki, S. *Chem. Lett.* **1993**, 2099−2102.
(9) Whittaker, M. M.; Chuang, Y-Y.; Whittaker, J. W. *J. Am. Chem. Soc.* **1993**, *115*, 10029−10035.
(10) Adams, H.; Bailey, N. A.; Fenton, D. E.; He, Q.; Ohba, M.; Okawa, H. *Inorg. Chim. Acta* **1994**, *215*, 1−3.

0020-1669/96/1335-0382$12.00/0 

**Syntheses. 2-(Methylthio)-*p*-cresol (mtc)** was synthesized according to a published procedure,[11] and its structure was confirmed by mass spectrometry and NMR spectroscopy.[9]

**2,2′-Bis(methylthio)-6,6′-bi-*p*-cresol ((mtc)$_2$).** (Methylthio)cresol dimer was prepared as previously described,[9] isolated by acidification of [Cu(PMDT)(((methylthio)cresol)$_2$)](ClO$_4$), and purified by silica gel chromatography.

**2-Hydroxy-3,5-dimethyl-benzaldehyde** was synthesized by a modification of the Reimer−Tiemann reaction.[12−14] A mixture of 83 mL of 2,4-dimethylphenol and 4.2 mL of triethylamine in 350 mL of chloroform was added dropwise to 800 mL of 50% NaOH in water at 75 °C with vigorous stirring under reflux. The reaction mixture was acidified with 110 mL of concentrated HCl. After addition of sufficient water to dissolve the salt, the dark oil layer was collected and the product extracted with $CH_2Cl_2$. After evaporation of solvent, the product was purified by steam distillation, silica gel chromatography, and bisulfite reaction.[15] The overall yield after release from the bisulfite complex was approximately 20%. The compound was characterized by NMR ($\delta$ 2.24, 2.30, 5.30, 7.17, 7.22, 9.83, 11.08) and mass spectrometry ($M^+ = 150$). Anal. Calcd for hydroxydimethylbenzaldehyde, $C_9H_{10}O_2$: C, 71.99; H, 6.71. Found: C, 71.90; H, 6.68.

**3-(Methylthio)-2,5-cresotaldehyde** was synthesized using modified Reimer−Tiemann reaction conditions.[12−14] A 2 g sample of 2-(methylthio)-*p*-cresol was added to 10 g of KOH in 10 mL of water under argon with vigorous stirring, followed by a mixture of 15 mL of $CHCl_3$ in 200 mL of benzene. The reaction mixture was refluxed at 48 °C with vigorous stirring for 10 h. After cooling, the reaction mixture was extracted twice with water (150 mL total volume). The water layer was neutralized with 10% $H_2SO_4$ and the product extracted with $CH_2Cl_2$ and dried over anhydrous $Na_2SO_4$. The reaction product was identified by fluorescent silica gel TLC using hexane/ethyl acetate (9:1) solvent. Further purification by silica gel chromatography with hexane/ethyl acetate yielded a crystalline product after evaporation of the solvent and cooling to −20 °C. Final overall yield: 5−10%. 3-(Methylthio)-2,5-cresotaldehyde was characterized by NMR ($\delta$ 2.35, 2.45, 7.19, 7.26, 11.36, in $CDCl_3$) and mass spectrometry ($M^+ = 182$). Anal. Calcd for (methylthio)cresotaldehyde, $C_9H_{10}O_2S$: C, 59.34; H, 5.49. Found: C, 59.37; H, 5.71.

**(2-Pyridylmethyl)[(2-hydroxy-3,5-dimethylphenyl)methyl][(2-hydroxy-5-methyl-3-(methylthio)phenyl)methyl]amine (dnc = duncamine).** A 0.5 g sample of 3-(methylthio)-2,5-cresotaldehyde in dry methanol was stirred under anaerobic conditions, and 1 equiv of 2-(aminomethyl)pyridine was added. After formation of the Schiff base, 1 equiv of sodium cyanoborohydride[16] and 1 equiv of freshly prepared anhydrous HCl in dry methanol were added dropwise to the reaction mixture. The solution was stirred for 3 h under argon, after which 1 equiv of dimethylhydroxybenzaldehyde bisulfite compound[15] was added and the reaction was continued for 3 d under a $CaSO_4$ drying tube. A white precipitate was filtered off, and the solvent was evaporated yielding an oil-like filtrate that was separated from a salt precipitate and diluted with 25 mL of methanol. The product crystallized over several days. Yield: approximately 40%. The compound was characterized by NMR ($\delta$ 2.20, 2.27, 2.43, 3.82, 6.69, 6.74, 6.89, 6.96, 7.15, 7.32, 7.75, 8.71, in $CDCl_3$) and mass spectrometry ($M^+ = 408$). Anal. Calcd for this compound, $C_{24}H_{28}N_2O_2S$: C, 70.59; H, 6.86; N, 6.86. Found: C, 69.43; H, 6.95; N, 6.61.

**The Copper Complex ([Cu$_2$(dnc)$_2$]·2CH$_3$CN).** Tetrakis(acetonitrile)copper(II) tetrafluoroborate ([Cu(CH$_3$CN)$_4$](BF$_4$)$_2$) was synthesized according to published procedures.[17,18] One equivalent of duncamine was treated with 2 equiv of tetramethylammonium hydroxide in CH$_3$CN prior to addition of 1 equiv of [Cu(CH$_3$CN)$_4$](BF$_4$)$_2$ in CH$_3$CN. Dark brown crystals formed after several days.

**Table 1.** Summary of Crystal Data for Cu$_2$(dnc)$_2$·2NCCH$_3$ (dnc = (CH$_2$C$_6$H$_2$(CH$_3$)$_2$O)(CH$_2$C$_6$H$_2$(SCH$_3$)(CH$_3$)O)(CH$_2$C$_5$H$_4$N)N)[a]

| | |
|---|---|
| fw | 1022.2 |
| crystal system | triclinic |
| space group | $P\bar{1}$-$C_i^1$ (No. 2) |
| $a$, Å | 14.740(7) |
| $b$, Å | 11.378(4) |
| $c$, Å | 15.633(6) |
| α, deg | 93.08(3) |
| $\beta$, deg | 101.95(3) |
| $\gamma$, deg | 92.28(3) |
| $V$, Å$^3$ | 2558(2) |
| $Z$ | 2 |
| $d_{calc}$, g/cm$^3$ | 1.327 |
| radiation $\lambda$, Å | 0.710 73 (Mo Kᾱ) |
| $\mu$, mm$^{-1}$ | 0.96 |
| $T$, K | 293 ± 1 |
| transm factors | 0.810−1.000 |
| total no. of reflns collected | 7936 |
| no. of indept reflns collected | 7613 |
| $R_{int}$ | 0.026 |

[a] All calculations were performed on a Data General Eclipse S-200 or S-230 computer using versions of the Nicolet E-XTL or SHELXTL interactive crystallographic software package or on a DEC Microvax II computer or an IBM compatible 486 personal computer using the Siemens SHELXTL-PLUS or SHELXTL-PC interactive software package as modified at Crystalytics Co.

**X-ray Crystallography.** Single crystals of [Cu$_2$(dnc)$_2$]·2NCCH$_3$ are, at 293 ± 1 K, triclinic, of space group $P\bar{1}$-$C_i^1$ (No. 2), with $a$ = 14.740(7) Å, $b$ = 11.378(4) Å, $c$ = 15.633(6) Å, α = 93.08(3)°, $\beta$ = 101.95(3)°, $\gamma$ = 92.28(3)°, $V$ = 2558(2) Å$^3$, and $Z$ = 2 {$d_{calcd}$ = 1.327 g cm$^{-3}$; $\mu_a$(Mo Kᾱ) = 0.96 mm$^{-1}$}. A total of 7613 independent reflections having $2\theta$(Mo Kᾱ) < 47.2° (the equivalent of 0.65 limiting Cu Kᾱ spheres) were collected on a computer-controlled four-circle Nicolet (Siemens) autodiffractometer using full (1.00°-wide) $\omega$ scans and graphite-monochromated Mo Kᾱ radiation. Crystal parameters and the details of the data and reduction are given in Table 1. The structure was solved using direct-methods techniques with the Siemens SHELXTL-PC software package as modified by Crystalytics, Inc. The resulting structure parameters were refined to convergence {$R_1$(unweighted, based on $F$) = 0.053 for 2505 independent absorption-corrected reflections having $2\theta$(Mo Kᾱ) < 47.2° and $I > 3\sigma(I)$} using counter-weighted full-matrix least-squares techniques and a structural model which incorporated anisotropic thermal parameters for all non-hydrogen atoms and isotropic thermal parameters for all hydrogen atoms. The eight methyl groups ($C_{7a}$, $C_{8a}$, $C_{7b}$, $C_{8b}$, $C_{7d}$, $C_{8d}$, $C_{7e}$, $C_{8e}$) and their hydrogens were refined as rigid rotors with sp$^3$-hybridized geometry and a C−H bond length of 0.96 Å. The initial orientation of each methyl group was determined from difference Fourier positions for the hydrogen atoms. The final orientation of each methyl group was determined by three rotational parameters. The refined positions for the rigid-rotor methyl groups gave S−C−H and C−C−H angles which ranged from 102 to 123°. The remaining hydrogen atoms were included in the structure factor calculations as idealized atoms (assuming sp$^3$- or sp$^2$-hybridization of the carbon atoms and a C−H bond length of 0.96 Å) "riding" on their respective carbon atoms. The isotropic thermal parameter of each hydrogen atom was fixed at 1.2 times the equivalent isotropic thermal parameter of the carbon atom to which it is covalently bonded. Details of the structure are given in Tables 2 and 3.

## Results and Discussion

**Coordination Chemistry.** The duncamine ligand is insoluble in water but dissolves readily in acetonitrile in the presence of 2 equiv of base. Addition of tetrakis(acetonitrile)copper(II) to the deprotonated duncamine ligand leads to formation of a dimeric complex that crystallizes from acetonitrile in thin blades that served for X-ray structure determination. The structure of the dinuclear complex (Figure 1) shows the two five-coordinated metal ions in roughly equivalent sites (not related by crystallographic symmetry) having distorted trigonal bipyramidal

(11) Pilgram, K. H.; Medina, D.; Solomay, S. B.; Gaertner, G. U. Method of production of hydroxyaryl thioethers from sulfonium compounds. U.S. Patent 3772391, 1973.
(12) Russell, A.; Lockhart, L. B. *Organic Syntheses*; Wiley: New York, 1955; Collect Vol. III, p 463.
(13) Sasson, Y.; Yonovich, M. *Tetrahedron Lett.* **1979**, *39*, 3753−3756.
(14) Wynberg, H.; Meijer, E. *Org. React.* **1982**, *28*, 1−36.
(15) Chattopadhyay, S. P.; Das, A. K. *J. Indian Chem. Soc.* **1986**, *63*, 256−259.
(16) Borch, R. F.; Bernstein, M. D.; Durst, H. D. *J. Am. Chem. Soc.* **1971**, *93*, 2897−2904.
(17) Hathaway, B. J.; Underhill, A. E. *J. Chem. Soc.* **1960**, 3705−3711.
(18) Hathaway, B. J.; Holah, D. G.; Underhill, A. E. *J. Chem. Soc.* **1962**, 2444−2448.

**Table 2.** Bond Distances (Å) Involving Non-Hydrogen Atoms in Crystalline $Cu_2(dnc)_2 \cdot 2NCCH_3$[a,b]

| | | | |
|---|---|---|---|
| $Cu_1 \cdots Cu_2$ | 3.054(2) | | |
| $Cu_1-O_{1a}$ | 1.887(10) | $Cu_2-O_{1d}$ | 1.878(10) |
| $Cu_1-O_{1b}$ | 1.949(9) | $Cu_2-O_{1b}$ | 1.942(8) |
| $Cu_1-O_{1e}$ | 1.972(8) | $Cu_2-O_{1e}$ | 1.941(9) |
| $Cu_1-N_1$ | 2.143(11) | $Cu_2-N_2$ | 2.141(11) |
| $Cu_1-N_{1c}$ | 2.189(13) | $Cu_2-N_{1f}$ | 2.155(11) |

[a] The numbers in parentheses are the estimated standard deviations in the last significant digit. [b] Atoms are labeled in agreement with Figure 1.

**Table 3.** Bond Angles (deg) Involving Non-Hydrogen Atoms in Crystalline $Cu_2(dnc)_2 \cdot 2NCCH_3$[a,b]

| | | | |
|---|---|---|---|
| $O_{1a}Cu_1O_{1b}$ | 168.6(4) | $O_{1d}Cu_2O_{1e}$ | 168.4(4) |
| $O_{1e}Cu_1N_1$ | 140.0(4) | $O_{1b}Cu_2N_2$ | 135.6(4) |
| $O_{1e}Cu_1N_{1c}$ | 137.1(5) | $O_{1b}Cu_2N_{1f}$ | 143.4(4) |
| $O_{1a}Cu_1O_{1e}$ | 94.2(4) | $O_{1b}Cu_2O_{1d}$ | 93.1(4) |
| $O_{1a}Cu_1N_1$ | 94.4(4) | $O_{1d}Cu_2N_2$ | 94.4(4) |
| $O_{1b}Cu_1N_1$ | 93.5(4) | $O_{1e}Cu_2N_2$ | 93.1(4) |
| $O_{1a}Cu_1N_{1c}$ | 99.9(5) | $O_{1d}Cu_2N_{1f}$ | 98.3(4) |
| $O_{1b}Cu_1N_{1c}$ | 89.7(4) | $O_{1e}Cu_2N_{1f}$ | 91.9(4) |
| $O_{1b}Cu_1O_{1e}$ | 74.5(4) | $O_{1b}Cu_2O_{1e}$ | 75.4(4) |
| $N_1Cu_1N_{1c}$ | 79.2(5) | $N_2Cu_2N_{1f}$ | 78.2(4) |

[a] The numbers in parentheses are the estimated standard deviations in the last significant digit. [b] Atoms are labeled in agreement with Figure 1.

geometry defined by *trans*-axial phenolate ligation with the shortest bond distances and by equatorial interactions from the tripod nitrogen, the pyridyl side chain of the chelate, and a phenolate bridge from the opposing chelate. The structure of the half-dimer complex as resolved by X-ray crystallography shown pictorially in structure **2** illustrates the basic pattern of

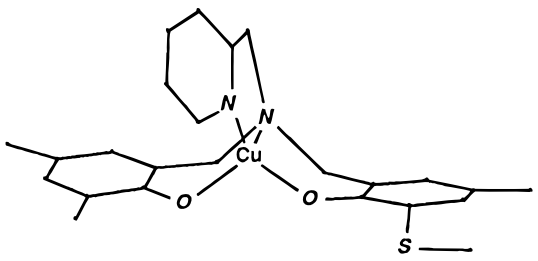


**2**

ligand interactions. In the dinuclear complex, the two Cu atoms are unsymmetrically bridged by oxygens from the phenolates of the dimethylphenol side chains, which are expected to be relatively basic compared to the thioether-substituted phenolate oxygens[9] and to encounter less severe steric constraints. This bridging arrangement forms a $Cu_2O_2$ core with short Cu−O bond distances (1.88−1.89 Å) for the $\mu$-bridging oxygens and a Cu−Cu separation of only 3.05 Å. Bis(phenolate)ligation for the dnc chelate appears to preferentially lead to *trans*-axial coordination geometry for the two distinct phenolates, rather than the mixed equatorial/axial ligation found for the two tyrosines (Y272 and Y495) in the native galactose oxidase enzyme complex.[7] The compressed *trans*-axial arrangement maximizes the Coulombic interactions between the anionic groups and the metal cation, making a favorable energetic contribution to complex stability from the ligand field point of view, suggesting that one role for the protein in galactose oxidase is to stabilize a relatively unfavorable geometry for the bis(tyrosinate) copper complex.

**Optical Absorption Spectra.** The interactions of the duncamine copper dimer with pyridine and other exogenous bases can be monitored by UV−vis absorption spectroscopy. The optical absorption spectrum of the dimeric complex in $CH_3CN$ is shown in Figure 2. Broad, intense absorption features ($\epsilon_{425}$ = 2545 $M^{-1}$ $cm^{-1}$ per Cu) dominating the solution spectrum are consistent with low-energy phenolate-to-copper ligand-to-metal charge transfer (LMCT) excitations in the bridged complex. Addition of pyridine results in a shift of the spectral features to lower energy and a decrease in the intensity ($\epsilon_{475}$ = 1430 $M^{-1}$ $cm^{-1}$ per Cu), reflecting dissociation of the dimer on coordination by base. The Cu(II) ligand field spectra exhibit a similar red shift (from 640 to 705 nm), consistent with a reduction in the axial ligand perturbation in the monomer. The affinity of exogenous ligand interactions measured by spectrophotometric titration yields an estimate of $K_D$ for the pyridine complex (1.95 mM). While other nitrogenous bases (quinuclidine and 3,5-lutidine) and fluoride or chloride ions similarly titrate the dimeric complex, no significant perturbation was detected using collidine (2,4,6-trimethylpyridine), presumably because of the steric constraints imposed by the *ortho* substitution pattern on addition to the chelate. The monomeric form of the pyridine adduct is demonstrated by the observation of a simple Cu(II) EPR signal for this complex (see below).

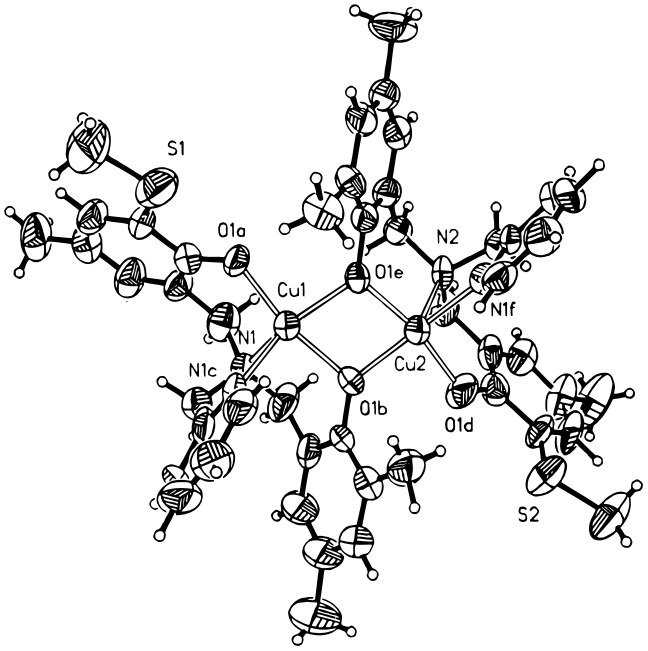


**Figure 1.** X-ray structure for $[Cu_2(dnc)_2] \cdot 2CH_3CN$. The diagram shows a perspective drawing of the structure of $Cu_2(dnc)_2$ in crystalline $Cu_2(dnc)_2 \cdot 2NCCH_3$ with non-hydrogen atoms represented by thermal vibration ellipsoids drawn to encompass 50% of their electron density. Hydrogen atoms are represented by arbitrarily-small spheres which are in no way representative of their true thermal motion.

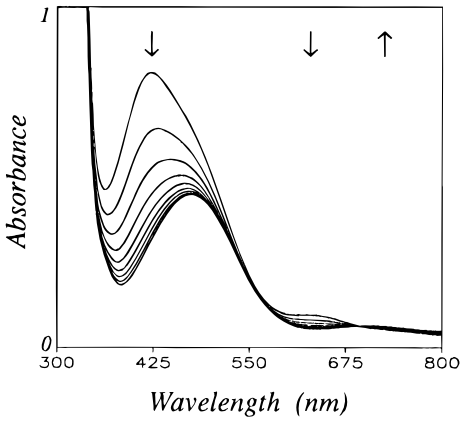


**Figure 2.** Titration of $[Cu_2(dnc)_2]$ by pyridine, for the copper complex (0.32 mM) in acetonitrile with addition pyridine to final concentrations of 0, 0.62, 1.23, 1.83, 2.48, 3.08, 3.70, 4.31, and 4.93 mM, respectively, for successive steps. Arrows indicate direction of absorption change with increasing pyridine concentration.

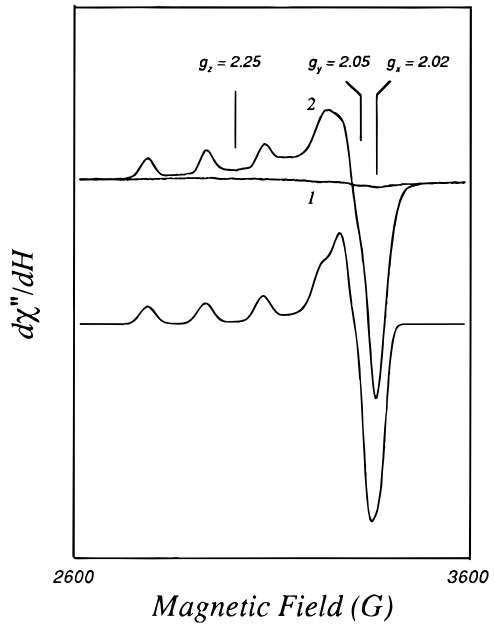


**Figure 3.** EPR spectra of $[Cu_2(dnc)_2]$ and its pyridine adduct. Top: 2.0 mM $[Cu_2(dnc)_2]$ in $CH_2Cl_2$ spectrum 1 and the same sample after addition of excess pyridine spectrum 2. Instrumental parameters: microwave frequency, 9.46 GHz; modulation frequency, 100 kHz; modulation amplitude, 10 G; microwave power, 1 mW; temperature, 120 K. Bottom: spectrum simulated using the parameters $g_x = 2.02$, $g_y = 2.05$, $g_z = 2.25$, $a_z$(Cu) = 150 G, and line width 40 G.

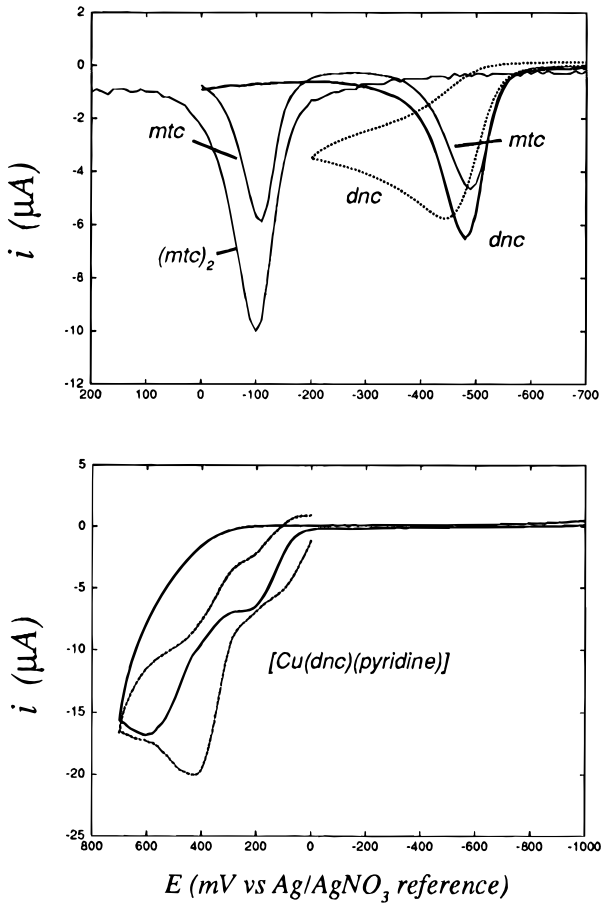


**Figure 4.** Electroanalytical characterization of the dnc ligand and its Cu complex. Top: (solid lines) comparison of square-wave voltammetric scans for 2-(methylthio)-*p*-cresol (mtc), the *o*,*o*′-linked (methylthio)cresol dimer ($(mtc)_2$), and the duncamine ligand (dnc) in $CH_2Cl_2$ containing tetrabutylammonium hydroxide and 0.1 M tetrabutylammonium tetrafluoroborate supporting electrolyte at a gold electrode; (broken line) cyclic voltammetry for the duncamine ligand under identical conditions. Bottom: cyclic voltammetry for [Cu(dnc)(pyridine)] in $CH_2Cl_2$ (solid line) and acetonitrile (dashed line) containing 0.1 M tetrabutylammonium tetrafluoroborate supporting electrolyte at a gold electrode.

The intense absorption band at 475 nm for the pyridine adduct is consistent with equatorial phenolate coordination in a pyramidal complex for the monomer and is comparable in both transition energy and intensity to phenolate LMCT previously reported for a simple Cu phenolate model compound ($\epsilon_{490}$ = 1360 $M^{-1}$ $cm^{-1}$ per Cu)[9]. The spectrum of the $Cu_2(dnc)_2$ dinuclear complex, on the other hand, more strongly resembles that of Cu(II) transferrin (bis(tyrosinate) coordination) ($\epsilon_{438}$ = 2400 $M^{-1}$ $cm^{-1}$ per Cu).[19] Since the thioether-substituted phenolate ligand contributes very little to the LMCT intensity in complexes,[9] the intensities roughly parallel the number of simple phenolate ligands bound. Mutation of the native structure of galactose oxidase substituting histidine for tryptophan in the active site (W290H) has been reported to result in unusual absorption spectra for the metal center ($\epsilon_{476}$ = 2800 $M^{-1}$ $cm^{-1}$ per Cu)[20] which are strikingly similar to the spectrum of the Cu(dnc) monomer described above. Since the mutant enzyme lacks catalytic activity and shows little change in absorption spectrum on treatment with ferricyanide,[20] it seems likely that replacement of tryptophan leads to a change in geometry at copper that stabilizes an inactive, bis(phenolate) complex in which formation of the radical is suppressed.

**EPR Spectroscopy.** Consistent with the strong antiferromagnetic exchange interactions expected for the $\mu$-bridged $Cu_2O_2$ core, no EPR signal can be detected for the dimer complex at low temperature (Figure 3). However, addition of an excess of coordinating base results in the appearance of EPR spectra arising from a simple Cu(II) center. Quantitation of this signal indicates complete conversion of the EPR-silent dimeric complex to a homogeneous paramagnetic product. The ground state parameters extracted from the experimental spectrum by simulation ($g_x = 2.02$, $g_y = 2.05$, $g_z = 2.25$; $a_z$(Cu) = 150 G), reflect a ligand environment of predominantly axial character with a small rhombic perturbation. Axial $g$ shifts of this magnitude are typical of a Cu(II) ion in pyramidal coordination stabilizing a $d_{x^2-y^2}$ orbital ground state, consistent with dissociation of the dimer on addition of aromatic amine forming a distorted pyramidal monomeric species containing the exogeous base (**2**). Similar ground state parameters have previously been obtained from low-temperature EPR spectra for the Cu(II) azide complex in galactose oxidase (2.25, 2.08, 2.02)[21] and a Cu(II) phenolate model compound (2.250, 2.065, 2.050).[9] The enzyme complex has a predominantly axial distortion as a result of pseudorotation of the metal center associated with ligand binding.[22]

**Ligand Redox Reactions.** Voltammetric analyses of the redox reactivity of a simple thioether-substituted phenol (2-(methylthio)-*p*-cresol, mtc), the *o*,*o*′-linked (methylthio)cresol dimer ($(mtc)_2$), and the complete duncamine ligand are shown in Figure 4 (top), and the data are given in Table 4. In cyclic voltammetry, the deprotonated free ligand exhibits a single quasireversible voltammetric wave at low potential with an anodic peak at −450 mV (vs $Ag/AgNO_3$ in $CH_3CN$), ap-

(19) Ainscough, E. W.; Brodie, A. M.; Plowman, J. E. *Inorg. Chim. Acta* **1979**, *33*, 149−153.
(20) Baron, A. J.; Stevens, C.; Wilmot, C.; Seneviratnes, K. D.; Blakeley, V.; Dooley, D. M.; Phillips, S. E. V.; Knowles, P. F.; McPherson, M. J. *J. Biol. Chem.* **1994**, *269*, 25095−25105.
(21) Whittaker, M. M.; Whittaker, J. W. *Biophys. J.* **1993**, *64*, 762−772.
(22) Landrum, G. A.; Ekberg, C. A.; Whittaker, J. W. *Biophys. J.* **1995**, *69*, 674−689.
(23) McGlashin, M. L.; Eads, D. D.; Spiro, T. G.; Whittaker, J. W. *J. Phys. Chem.* **1995**, *99*, 4918−4922.

**Table 4.** Electroanalytical Data

| compd | $E$, mV[a] in $CH_3CN$ | in $CH_2Cl_2$ | compd | $E$, mV[a] in $CH_3CN$ | in $CH_2Cl_2$ |
|---|---|---|---|---|---|
| mtc[b] | −472 | −395 | Cu(dnc)(py) | +116 | +234 |
| | −74 | −73 | | +463 | +580 |
| $(mtc)_2$[c] | −74 | −73 | Fc[e] | +91 | +180 |
| dnc[d] | −450 | −400 | | | |

[a] Anodic peak measured vs Ag/0.1 M $AgNO_3$ in $CH_3CN$ reference, using gold working electrode. [b] 2-(Methylthio)-*p*-cresolate. [c] *o*,*o*′-linked 2-(methylthio)-*p*-cresolate dimer. [d] Duncamine, $[(CH_2C_6H_2(CH_3)_2O)(CH_2C_6H_2(SCH_3)(CH_3)O)(CH_2C_5H_4N)N]$. [e] Ferrocene.

proximately matching the anodic current peak in the square-wave voltammetric scan. This low-potential redox step arises from the relatively easy oxidation of the thioether-substituted phenolic arm and matches the low-potential step (−472 mV) observed for oxidation of the simpler 2-(methylthio)-*p*-cresolate ion. The latter compound exhibits an additional wave at 400 mV higher potential that appears to result from secondary oxidation of the product of oxidative coupling of the phenoxyl radical formed in the first step. This assignment is confirmed by comparison with voltammetric data for the isolated dimer. The formation of the *o*,*o*′-linked dimer under mild conditions has been previously noted,[9] and the nearly equal amplitudes of the monomer and dimer current peaks in the square-wave voltammetric scan suggest that a significant fraction of molecules undergoing oxidation in the first step may react to form the dimer. In contrast, the free duncamine ligand is protected from dimerization by the aminomethyl side chain in the reactive *ortho* ring position and thus exhibits a single clean redox process in this potential range (Figure 4, top). Protonation of either the simple thioether compound or the complete duncamine ligand stabilizes the parent phenol, shifting the phenol/phenoxyl redox to potentials greater than +400 mV. Formation of the dimeric bridged dinuclear complex by Cu(II) coordination eliminates ligand redox chemistry in the potential range −1000 to +700 mV, except for small currents near +100 mV identical to those observed for the monomer complex (see below) but corresponding to only a fraction of the amplitude, probably representing a fraction of dimer that dissociates through interaction with the supporting electrolyte or solvent. Binding pyridine quantitatively converts the complex to the monomeric form, for which redox is observed at +100 mV (Figure 4, bottom), consistent with stabilization of phenolate in the metal complex compared to the free ligand, making the oxidation less favorable. Metalation thus parallels protonation in the redox chemistry of this ligand. Complex formation with the dianionic ligand also stabilizes the divalent metal ion, and no redox associated with the Cu(II) center is observed down to −1000 mV.

**Conclusions.** The active site of galactose oxidase is unusual in the extent to which ligand reactivity is involved in catalysis with both redox and acid/base roles for the two phenolate ligands (Y272 and Y495). Modeling this active site requires the assembly of a variety of functional groups in a specific geometric arrangement. The Borch reaction between bisulfite derivatives of aldehydes and primary or secondary amines[16] appears to be a versatile and effective approach to the synthesis of chelate systems including a variety of functional groups in a tripod ligand geometry, providing an alternative to the direct condensation of aldehydes and amines, which has proven effective in other tripod syntheses.[24] Using this approach, we have prepared an active-site analog for the metalloenzyme galactose oxidase based on a chelate system formed in a one-pot reaction from simple precursors, linking the three distinct arms in an ordered reaction that allows the controlled introduction of new functional groups.

The redox properties of both copper and the redox-active duncamine ligand clearly depend on the interactions within the complex. The bis(phenolate) coordination of the Cu−duncamine complex makes the thioether-substituted phenolate group more difficult to oxidize, shifting the redox potential at least +0.5 V in the metal complex compared to the free ligand, and the metal is likewise made more difficult to reduce with a dianionic ligand complement compared to copper coordinated by neutral pyridyl ligands.[24] The interplay between ligand and metal redox chemistry in the analog suggests that similar factors may be important in the biological complex. In particular, the fluxionality of the enzyme active site may have a role in determining the redox reactivity of the protein by controlling the basicity of the ligating groups. This fluxionality has previously been identified as a key feature of the catalytic complex, modulating the basicity of the simple tyosine phenolate (Y495 in **1**) through pseudorotation driven by the binding of exogenous ligands, permitting the phenolate to serve as a general base in catalysis.[25]

Even though the Cu−duncamine complex appears to contain the basic features of the copper binding site in galactose oxidase (**1**), its spectroscopic behavior is very different and it lacks catalytic activity. The optical spectra of the Cu(II) model (Figure 2) are distinct from those of the radical-containing, catalytically active enzyme (dominated by ligand-to-ligand charge transfer absorption of the radical complex[23]), more closely resembling the phenolate-to-copper LMCT spectra of the reductively inactivated Cu(II) enzyme.[4,23] The analog spectra even more closely resemble spectra reported for a mutant form of galactose oxidase in which the active-site tryptophan residue is replaced by histidine (W290H).[20] Crystallographic studies show that the reorganization of the metal binding site in the W290H protein is quite conservative;[20] in particular the same metal ligands are retained in the mutant complex, which is, however, catalytically inactive. The similarity between the optical spectrum of the inorganic model (which arises from strong bis(phenolate) interactions in low coordination number) and that of the W290H mutant suggests that the mutation changes the structure of the active-site complex sufficiently to alter the interactions between the two tyrosine phenolates and copper, thus affecting the redox reactivity of the complex.[21] The tryptophan residue (W290) thus appears to play an important role in defining the structure of the active-site copper complex in galactose oxidase. Comparison of the catalytically active enzyme structure with the inactive W290H mutant and duncamine model complex emphasizes that subtle changes in ligation can have dramatic effects on spectroscopic and catalytic properties. We are currently exploring further the effects of structural modifications of the ligand on the reactivity of the model.

**Acknowledgment.** This work was supported by the National Institutes of Health (Grant GM-46749).

**Supporting Information Available:** Lists of atomic coordinates, anisotropic thermal parameters, bond lengths, bond angles, torsion angles, and nonbonded distances and a unit cell packing diagram for $[Cu_2(dnc)_2]\cdot 2NCCH_3$ (18 pages). Ordering information is given on any current masthead page.

IC951116C

(24) Chuang, C.; Lim, K.; Chen, Q.; Zubieta, J.; Canary, J. W. *Inorg. Chem.* **1995**, *34*, 2562−2568.

(25) Whittaker, J. W. In *Metal Ions in Biological Systems*; Sigel, H., Sigel, A., Eds.; Marcel Dekker, Inc.: Basel, Switzerland, 1994; pp 315−360.